Radiated Emission Simulation of a RIT4

IEPC-2015-411／ISTS-2015-b-411

Presented at Joint Conference of 30th International Symposium on Space Technology and Science,
34th International Electric Propulsion Conference and 6th Nano-satellite Symposium
Hyogo-Kobe, Japan
July 4–10, 2015

Timo Baruth* and Rainer Thüringer†
University of Applied Sciences, Giessen, 35390, Germany

Peter J. Klar‡
University of Giessen, Giessen, 35392, Germany

Abstract: In this paper we present the numerical simulation of a radio-frequency ion thruster (RIT) to analyze its behavior in terms of the radiated emission. A commercially three-dimensional electromagnetic simulation software based on the finite integral technique is used. By applying Gaussian signal pulses to the connectors of coil and grid system we can obtain the resulting electromagnetic field distribution in a small volume around the thruster, in time domain. A Fast Fourier Transformation was used to transform the results into frequency domain. The radiated emission at discrete points in the far field was calculated with use of a numerical algorithm. A CAD model of a RIT4 is imported to show the method exemplarily. To verify the simulation we use a Gigahertz Transversal Electromagnetic Cell (GTEM cell). The results show maximum emission at frequencies of 632 MHz and 945 MHz, caused by a resonance in the thruster grid system visualized by the 3D tool.

Nomenclature

CST	= Computer Simulation Technology (numerical simulation software package)
FFT	= fast fourier transformation
FIT	= finite integral technique
$GTEM$	= gigahertz transversal electromagnetic cell
NHV	= negative high-voltage supply
PHV	= positive high-voltage supply
RFG	= radio-frequency generator
RIT	= radio-frequency ion thruster

*Research Assistant, Department of Electrical Engineering, and timo.baruth@ei.thm.de
†Professor, Department of Electrical Engineering, and rainer.thueringer@ei.thm.de
‡Professor, Institute of Experimental Physics I, and Peter.J.Klar@exp1.physik.uni-giessen.de

I. Introduction

Since their invention by Horst Loeb at the University of Giessen in 1962, radio-frequency ion thruster (RIT) have been used for commercial applications since the late 1990s. The scope covers material processing, as well as the propulsion of spacecraft. Especially for thruster operation the compliance to EMC standards like MIL-STD-461[1] is important. To ensure that the limits are not exceeded, measurements and tests have to be performed, which causes high effort and cost especially for the radiated emission[2,3]. Measurement is usually inappropriate to find the responsible source of high radiation, because superposition of many radiation sources (e.g. thruster, cables, electronic systems, external sources, etc.) is measured. Even if one can identify the interferer, it can be difficult to isolate the components characteristic, being responsible for the radiation.

In this paper we present a method to analyze the characteristic of a electrical passive component in terms of radiated emission; characteristic means the radiation behavior over a defined frequency range. We can have a look on both, the possibility to characterize the components without other interfering components and on the electromagnetic field distribution inside the component to identify radiation sources.

A commercial 3 dimensional simulation software, provided by CST - Computer Simulation Technology[4], is used therefore. A CAD model of the component can be implemented and simulated in a definable frequency range. The result of the characterization process is a transfer function, that interlinks the electric input signal to the radiated emission. We show the characterization with a RIT4, exemplary.

II. Simulation method

The simulation method is illustrated in Fig.1. We use a full 3 dimensional simulation to determine the behavior of the thruster in terms of the radiated emission over the full frequency range. This simulation is done in time domain by applying Gaussian-shaped impulses as an excitation signal to the coil and grid system connectors (s. II.A). The electric and magnetic fields $\vec{E}$ and $\vec{H}$ are calculated with the Finite Integral Technique[5] in the hole simulation volume V for every time step. They will be recorded at the boundaries of the simulation domain ∂V and used to calculate the electromagnetic field distributions at discrete points in the far field (radiated emission) of the thruster (s. II.B). Afterwards transfer functions are build, with the Gaussian-shaped impulses as the input parameter and the far field emission as the output parameter. The transfer functions will be transformed into frequency domain to show the behavior in frequency domain. As a consequence the transfer function describes the effect of an input signal at a thruster connector on the radiation at a discrete point away from the RIT as a black-box model over the full frequency range. The hole computation process has to be execute only one time, because the time domain representation covers the hole frequency range of interest (s. II.A).

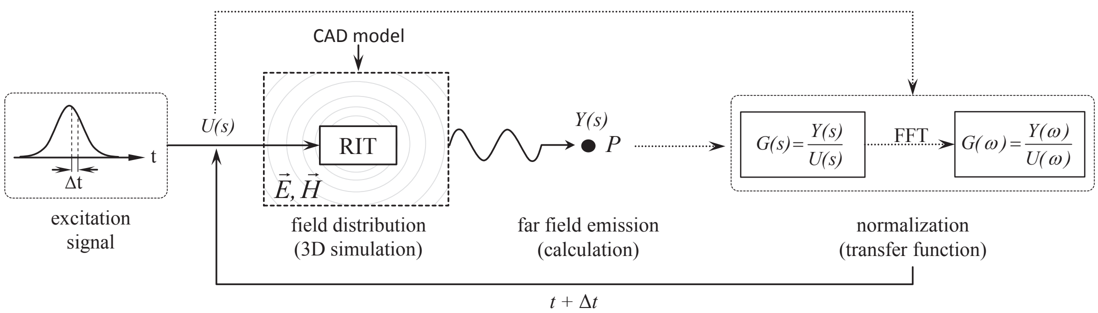

Figure 1. Schematic representation of the simulation process.

The next sections will describe the major elements of the process in more detail, to get a better understanding of how the simulation works.

A. Time domain simulation

Usually, analysis is done in frequency domain for EMC issues, because one is interested in the interference on a specific bandwidth, for instance. Because the model should cover a defined frequency range, this would mean to run the simulation several times at consecutive discrete points in the spectrum, to cover all frequencies of interest.

In this work we use a 3D simulation that works in time domain to calculate the field distribution inside the simulation domain. This approach has a fundamental advantage in contrast to the frequency domain approach. All frequencies, the time domain excitation signal include in its spectrum are also included in the results, inherently. To perform the EMC analysis, a Fast Fourier Transformation (FFT) transforms the results into frequency domain. This approach reduce the overall simulation time, because only one simulation run is needed to cover the entire spectrum of interest.

A suitable excitation signal is a Gaussian-shaped impulse (s. Fig.2). The impulse can be expressed by

$$x(t) = A \cdot e^{-\pi(t/\Delta t)^2} \tag{1}$$

where A is the amplitude, t the time variable and Δt the equivalent impulse duration. The equivalent impulse duration corresponds to the duration of a rectangular impulse with the same amplitude and surface as the Gaussian impulse. The pulse spectrum

$$X(f) = A \cdot \Delta t \cdot e^{-\pi(f \cdot \Delta t)^2} \tag{2}$$

(where f is the frequency) has analogous properties to $x(t)$ without any nulls in the spectrum, which is the key feature. The equivalent bandwidth Δf is linked to Δt by the reciprocity law

$$\Delta t \cdot \Delta f = 1 \tag{3}$$

which result in $\Delta t = 1$ ns for $\Delta f = 1$ GHz, exemplary.

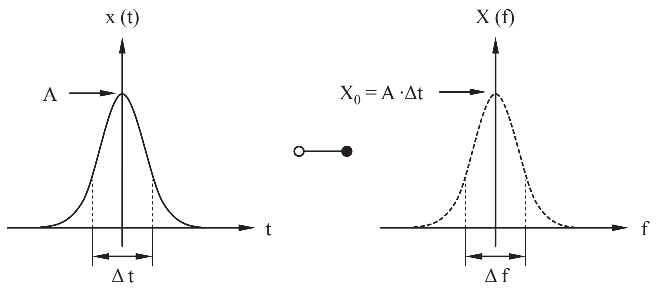

Figure 2. Gaussian-shaped impuls in time and frequency domain.

Because the discret frequencies in the spectrum of the Gaussian-shaped impulse are excited with different amplitudes (cf. Fig.2 *right*), there is a necessity to normalize the output signal ($Y(s)$ acc. to Fig. 1) on the excitation signal ($U(s)$ acc. to Fig. 1). That ensures, the effect of every frequency on the calculated emission value is rated correctly.

B. Far field calculation

In our approach, the software use the field distribution on the boundaries of the simulation domain to calculate the radiated emission. This is necessary, because the quantity of cells in the simulation domain is limited by the performance of the computer system. For the sufficient resolution of the field distribution inside the thruster and a small volume around, all cells are needed for calculation.

To validate this approch, the basic principle – based on Huygens principle[6] – is described in the following. According to Fig. 3a we assume a source S inside the simulation domain V_1 with its boundary ∂V, that generates the field distributions inside V_1 and in the outside V_2. The electric and magnetic fields immediately adjacent to the inside of the boundary are subscripted by number 1 (E_1, H_1), whereas the subscript 2 indicates

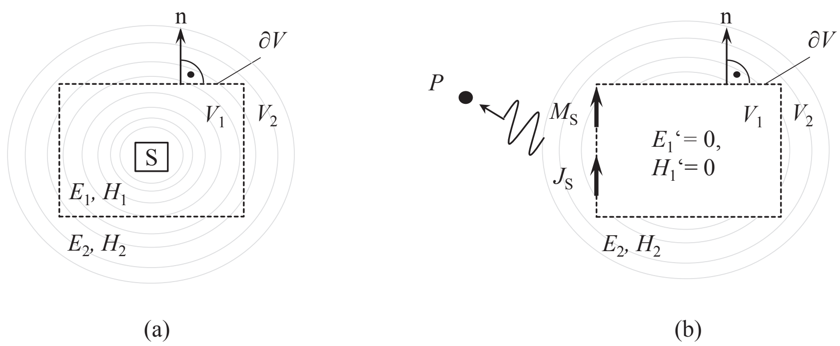

Figure 3. Schematic representation of the far field calculation procedur.

the fields just on the other side of ∂V (E_2, H_2). The character n indicates the normal to the boundary, pointing toward V_1.

Because the tangential field components are continuous on the boundary, there are no surface currents.

$$n \times (E_2 - E_1)|_{\partial V} = 0 \qquad and \qquad n \times (H_2 - H_1)|_{\partial V} = 0 \tag{4}$$

As visualized in Fig. 3b, one can describe the field outside the simulation domain with a magnetic surface current M_S – which is only a auxiliary quantity – and an electric surface current J_S by choosing the fields in V_1 to be zero[7]

$$n \times (E_2 - E_1') = -M_\mathrm{S} \qquad \Rightarrow \qquad n \times E_2 = -M_\mathrm{S} \tag{5}$$

$$n \times (H_2 - H_1') = J_\mathrm{S} \qquad \Rightarrow \qquad n \times H_2 = J_\mathrm{S} \tag{6}$$

Both expressions are equivalent but does not represent the former field distribution in V_1. For this application this is sufficient, being interessted in the field V_2 only.

In principle, a flowing current can be a radiating source (antenna), which is describable with the theory of the Hertzian electric dipole and can be used to calculate the fields in V_2. According to $PAUL$[8], the electric fields of a Hertzian electric dipole are given by

$$\hat{E}_\mathrm{r} = 2\frac{\hat{J}dl}{4\pi}\eta_0\beta_0\cos\theta\left(\frac{1}{{\beta_0}^2r^2} - j\frac{1}{{\beta_0}^3r^3}\right)e^{-j\beta_0 r} \tag{7}$$

$$\hat{E}_\theta = \frac{\hat{J}dl}{4\pi}\eta_0\beta_0\sin\theta\left(j\frac{1}{\beta_0 r} + \frac{1}{{\beta_0}^2r^2} - j\frac{1}{{\beta_0}^3r^3}\right)e^{-j\beta_0 r} \tag{8}$$

$$\hat{E}_\phi = 0 \tag{9}$$

in spherical coordinates. The indices of the electric field denotes their direction. The radial distance from origin to a point P is labeled with r, the angle between z axis and a radial line is θ and ϕ is the angle between x axis and y axis. $\hat{J}$ is a phasor current on the infinitesimal current element of length dl. In our case it is the current crossing the boundary. The intrinsic impedance of free space is η_0 and β_0 is given as $2\pi/\lambda_0$, where λ_0 is the wavelength at the frequency of the antenna current.

As pointed out in $PAUL$[8], the $1/r^3$ and $1/r^2$ terms are dominating at very close distances to the antenna, which is called the near field. At distances far away from the antenna (far field), the $1/r$ term dominates. The boundary between both regions is not meant to be a precise criterion, but is only intended to indicate a general region. In the software implementation of the calculation one assume far field conditions. As a consequence $\hat{E}_r$ can be neglected, likewise the $1/r^3$ and $1/r^2$ terms in Eqn. 7. Hence, the calculation is simplified to

$$\hat{E}_{\theta,\mathrm{ff}} = \frac{\hat{J}dl}{4\pi}\eta_0\sin\theta j\frac{1}{\beta_0 r}e^{-j\beta_0 r} \tag{10}$$

under far field conditions, which is denoted by the index ff.

To evaluate the distances where one can expect correct results, the field distribution of $\vec{E}$ and $\vec{H}$ at the simulation domain boundary ∂V are recorded and used them as an excitation (identifier: near field source) in another simulation (Fig. 4).

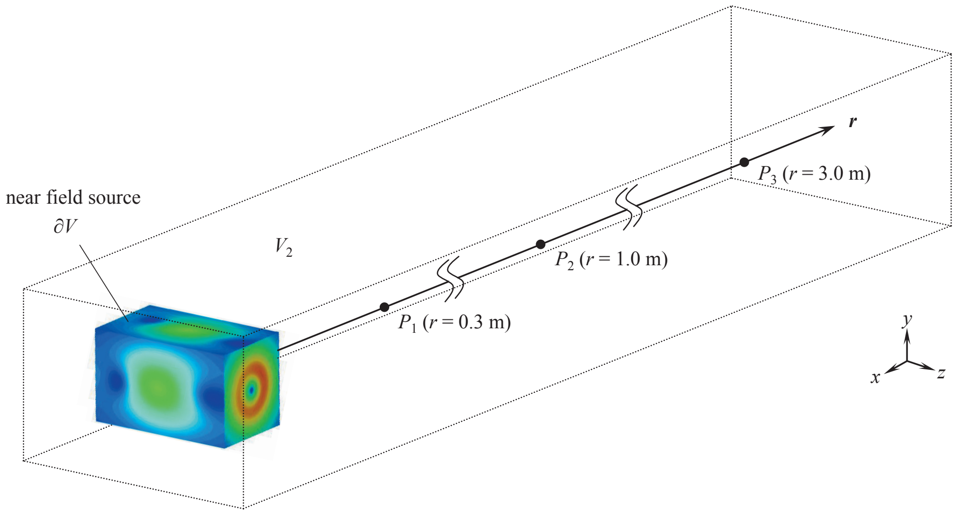

Figure 4. Setup for the field region evaluation.

Here we evaluated the resulting fields at distances of 0.3 m, 1.0 m and 3.0 m on the x axis. This is in contrast to the former described process. Now the fields at the evaluation points are not mathematically calculated as outlined above, but directly simulated in the new simulation domain V_2. This is possible, according to the maximum number of cells available for the simulation domain, because there is no need to simulate the hole thruster by taking the fields on ∂V from a former simulation.

The results are visualized in Fig. 5, where the identifier *far* labels the curves that only consider the $1/r$ term of $\hat{E}_\theta$, whereas the identifer *near* labels the curves that consider all $1/r^x$ terms.

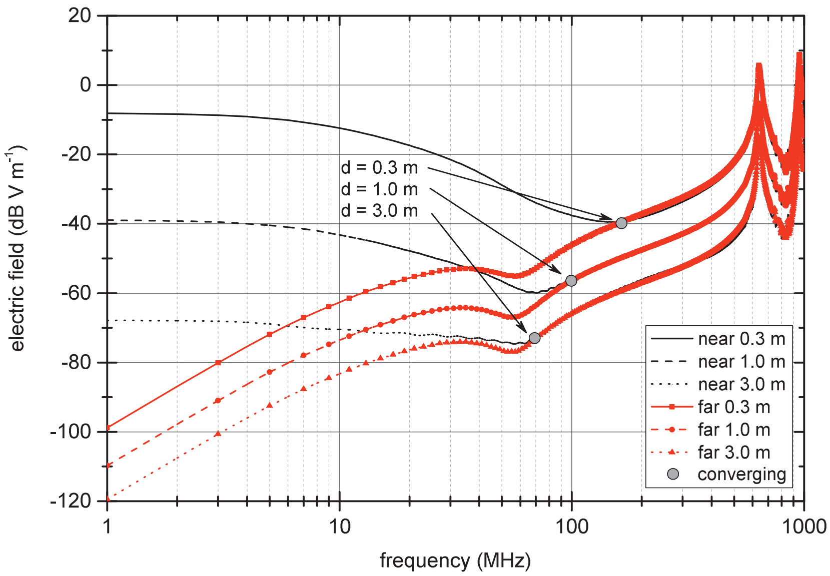

Figure 5. Results for the field region evaluation.

Obviously, the curves for the near fields and far fields match at certain frequency points. The frequency where the matching occurs is depending on the distance to the measurement point. For higher distances the curves converge at lower frequency points. This is due to the fact, that the far field region is also depending on the frequency and the wavelength respectively[6,7].

In consequence for our simulation approach the results of the calculated radiated emission are only valid at a sufficient distance from our model depending on the frequency. To ensure that the calculated results are correct for a distance of 3 m we can only rely on those results greater 70 MHz. Being in the near field for lower frequencies we probably will have misleading results.

III. Charaterization of a RIT4

A. Simulation model

With the described simulation method we have characterized a RIT4 in terms of radiated emissions. Therefore the CAD model of the thruster is implemented as shown in Fig. 6b. The thruster has four connectors which is also illustrated in the figure. They are labeled with RF for the radio-frequency input, NHV for the negative high voltage input, PHV for the positive high voltage input and GND for the electric reference. The behavior of all inputs were characterized separately.

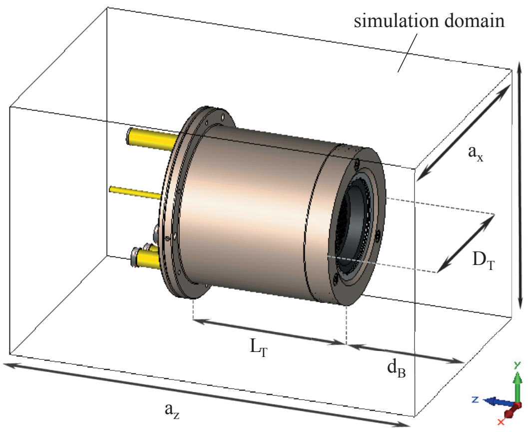

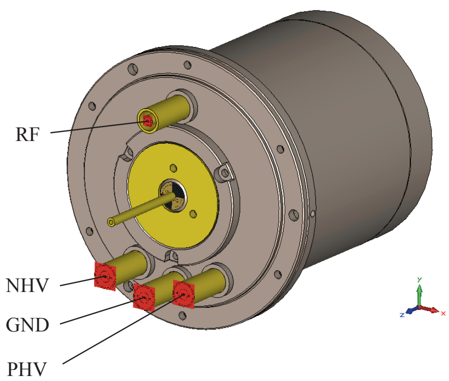

Figure 6. CAD model of the applied RIT4.

In Fig. 6a the dimensions of the thruster and the simulation domain are shown. The RIT4 has the following dimensions: $L_{\mathrm{T}} = 100$ mm, $D_{\mathrm{T}} = 83$ mm. The dimensions of the simulation domain are: $a_{\mathrm{x}} = 140$ mm, $a_{\mathrm{y}} = 140$ mm, $a_{\mathrm{z}} = 177$ mm and $d_{\mathrm{B}} = 20$ mm. The distance for the far field calculation is 3 m along the x axis.

B. Verification

To verify the calculated emission with the simulation approach, we used a GTEM cell. In principle a GTEM cell is a pyramid-shaped widened coaxial cable, which represents a electromagnetically insulated volume to the outside. When putting a radiating source between its inner conductor (septum) and its outer conductor, one can measure a voltage at the feeding point that is proportional to the emitted field of the source. The measured voltage can be correlated to a equivalent field strength at 3 m or 10 m distance for instance, which is due to corresponding standards like MIL-STD-461[1]. The correlation algorithm we used is implemented in MATLAB[9] and based on the mathematical description in *WILSON*[10]. This algorithm is valid for frequencies in a range from 30 MHz to 2.7 GHz.

For verification the GTEM cell is used in connection with a type N9000A spectrum analyzer. This spectrum analyzer includes also a tracking generator, which is used as the excitation source for the thruster. The measurement principle is shown in Fig. 7. The tracking generator is connected to the electrical ports of the thruster via a coaxial cable and a feed-through. It works as a sweep generator, which creates a sinus with a linearly varying frequency (0.03 to 1000 MHz) and a constant amplitude. This is the key feature

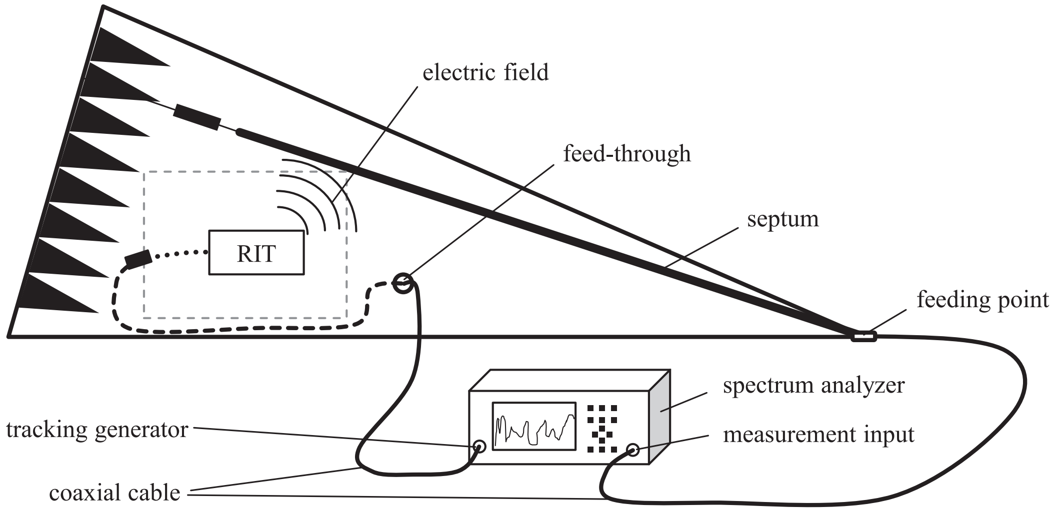

Figure 7. Schematic representation of the measurement with a GTEM cell.

of the verification, because the simulation results are normalized to the same constant amplitude of $1\sqrt{W}$. If the RIT radiates emissions at certain frequencies, they couple in the septum and will be measured with the spectrum analyzer. A measurement sequence is performed for every port of the RIT (RF, GND, NHV, PHV).

C. Results & Analysis

The results of simulation and verification measurement are shown in Fig. 8, for every connector separately. The simulation result is always represented by the solid line, whereas the dotted line is a reference measurement that shows the influence of the coaxial cable inside the GTEM cell. The measurement of the thruster in combination with the coaxial cable is shown as dash dotted lines.

Looking at the simulation results, one can see a successive increase from the lower frequency region up to the higher region around 600 MHz in all cases. The strong decrease at the lowest frequencies around 0 to 70 MHz can be ignored, because the calculation is not valid in this range (s. II.B). There are also two distinctive peaks in the spectrum at 632 MHz and 945 MHz.

With reference to the former mentioned possibility to look on the electromagnetic field distribution inside the thruster, one can now localize the radiation source. We used a so-called field monitor in frequency domain at 632 MHz as shown in Fig. 9. This monitor displays the electric field on a two dimensional plane. When placing this 2D plane on a position between the grid system, one can see that the field distribution is very similar to that of a dipole[6]. This is because the geometrical structure of the grid system causes a resonance for the frequency around 632 MHz. The same radiation mechanism works for a frequency of 945 MHz.

For the verification measurement one first have to take a look on the influence of the coaxial cable. In the cases b-d of Fig.8, the radiation up to 300 MHz is mainly caused by the cable. Only at higher frequencies the emission is dominated by the thruster radiation. Simulation and measurement show the same behavior in principle. One have to pay attention on the fact, that the GTEM cell causes resonances, which can be seen in the measurement results but not in the simulation results.

In case a of Fig. 8 – with the excitation signal at the RF connector – the emission is fully dominated by the combination of thruster and cable. The results are remarkable above those of the simulation. This is related to the fact, the simulation model is different to the real thruster at the RF connector. In the simulation model, the connector is shielded, like the GND, NHV, and PHV connectors. In the measurement the shielding is not existing, because we use a simple coaxial cable, not a triaxial cable.

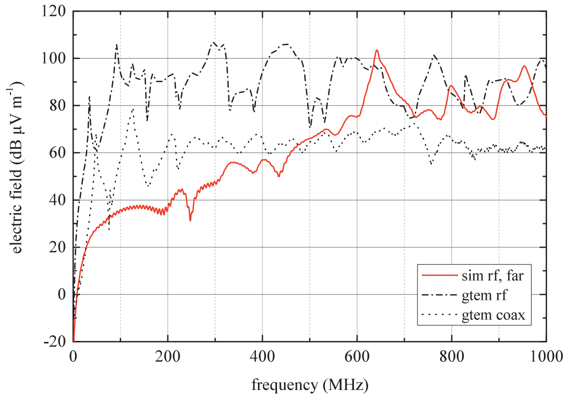

(a) RF

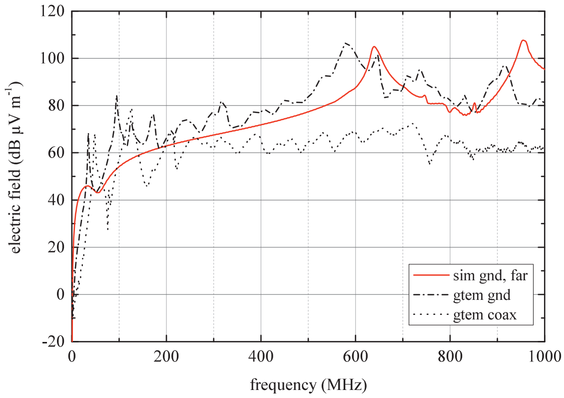

(b) GND

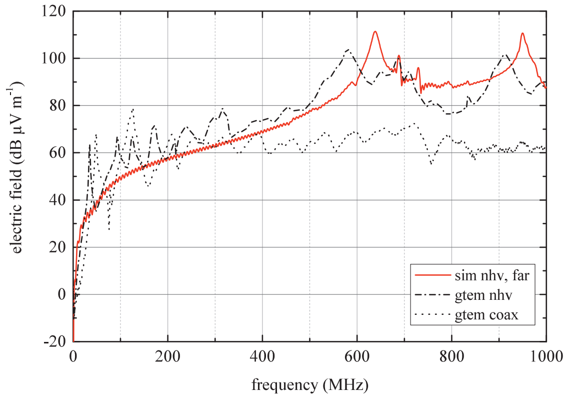

(c) NHV

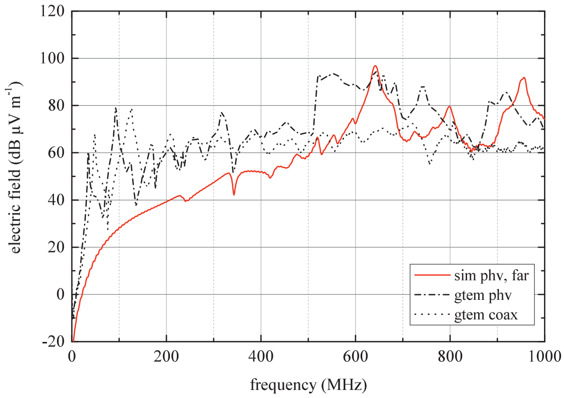

(d) PHV

Figure 8. Results of the simulated and measured radiated emission of a RIT4 with a constant excitation amplitude over frequency.

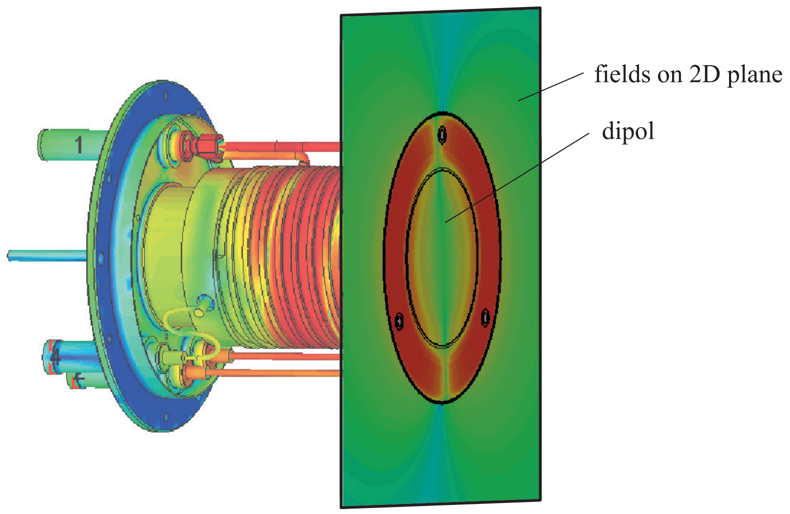

Figure 9. Visualization of the electric field strength on a 2D plane.

IV. Conclusion

A simulation method was presented to characterize passive components in terms of their radiated emission over a defined frequency range. Therefore a time domain simulation was used to compute the electromagnetic field distribution. Subsequently the resulting electric field strength in the far field has been calculated with a mathematical algorithm. The method was used for the characterization of a RIT4, exemplary.

A verification was done by GTEM cell measurements. A comparison of simulation results and measurement data show the same principle behavior for an excitation at the GND, NHV, and PHV connector. The results with use of the RF connector show large variations, due to a difference in the simulation model and the real thruster.

Finally, the motivation using a 3 dimensional simulation tool, to identify radiation sources inside a structure, could be confirmed.

V. Outlook

To make the model more realistic, a plasma material has to be implemented and verified. Because the simulation of the plasma itself is a challenging task, an independent algorithm[11] is available to obtain the relevant plasma parameter. These parameter can be used to define a material with a corresponding conductance, for instance.

For extending the model for near field issues, a method has to be found to validate the field distribution in the lower frequency region.

This might be of interest, because only signals in the frequency range of a few megahertz are used, for typical RIT operation. A promising approach can be near field probes.

The described method will be transferred to other components of a RIT system, for characterizing e.g. cables and electronic devices in terms of radiated emission, as well.

References

[1]U.S. Department of Defense, *MIL-STD-461F - Requirements for the Control of Electromagnetic Interference Characteristics of Subsystems and Equipment*, Dez 2007

[2]Ley, W., Wittman, K., and Hallmann, W., Handbook of Space Technology, AIAA, 2009

[3]Mueller, H., Kukies, R., and Bassner, H., "EMC tests on the RITA Ion Propulsion Assembly for the ARTEMIS satellite," *AIAA, SAE, ASME, and ASEE, Joint Propulsion Conference and Exhibit*, 28th, Nashville, TN, July 6-8, 1992. 7 p.

[4]CST Studio Suite 2015, Release Version 2015.01, CST - Computer Simulation Technology AG, 2015.

[5]Clemens, M., and Weiland, T., "Discrete Electromagnetism with the Finite Integration Technique," *Progress In Electromagnetice Research*, PIER 32, 2001, pp. 65-87.

[6]Kraus, John D., and Marhefka, Ronald J., *Antennas: For all Applications*, 3rd ed., McGraw-Hill, New York, 2003.

[7]Kark, Klaus W., *Antennen und Strahlungsfelder*, Vieweg+Teubner, Wiesbaden, Germany, 2010.

[8]Paul, Clayton R., *Introduction to electromagnetic compatibility*, John Wiley & Sons, Inc., 1992.

[9]MATLAB, Vers. 2013a, The Mathworks, 2013.

[10]Wilson, P., "On Correlating TEM Cell and OATS Emission Measurement," *IEEE Transactions On Electromagnetic Compatability*, Vol. 32, No. 1, Feb. 2001.

[11]Volkmar, C., and Ricklefs, U., "Implementation and Verification of a Self-Consistent 1D/3D Hybrid Performance and Impedance Model of Gridded Radio-Frequency Ion Thrusters," *Eur. Phys. J. D*, under review, 2015.